

## Correlated electron-nuclear dynamics in ultrafast photoinduced electron-transfer reactions at dye-semiconductor interfaces

Michael Thoss,<sup>1</sup> Ivan Kondov,<sup>1,\*</sup> and Haobin Wang<sup>2</sup>

<sup>1</sup>*Department of Chemistry, Technical University of Munich, D-85748 Garching, Germany*

<sup>2</sup>*Department of Chemistry and Biochemistry, MSC 3C, New Mexico State University, Las Cruces, New Mexico 88003, USA*

(Received 22 February 2007; revised manuscript received 30 July 2007; published 26 October 2007)

The correlated electron-nuclear dynamics in ultrafast photoinduced electron-transfer processes at dye-semiconductor interfaces is investigated, employing accurate quantum dynamical calculations. It is shown that—depending on the relative time scale of electronic and nuclear dynamics—electronic-vibrational coupling in dye-semiconductor systems may result in electron transfer driven by coherent vibrational motion, nuclear dynamics induced by ultrafast electron-transfer processes, as well as localization of the electron at the dye molecule.

DOI: [10.1103/PhysRevB.76.153313](https://doi.org/10.1103/PhysRevB.76.153313)

PACS number(s): 34.70.+e, 73.20.-r, 73.40.-c, 82.53.-k

Electron-transfer (ET) reactions play a fundamental role in many physical, chemical, and biological processes.<sup>1,2</sup> Important examples include ET in photosynthetic reaction centers of bacteria and plants,<sup>2,3</sup> photoinduced ET reactions in donor-acceptor complexes in solution,<sup>4</sup> as well as electron transport through single molecules covalently bound to metal leads in molecular electronics.<sup>5</sup> Among the great variety of different types of ET reactions, the process of electron injection from an electronically excited state of a dye molecule to a semiconductor substrate has received much attention in recent years both experimentally<sup>6–13</sup> and theoretically.<sup>14–20</sup> This interfacial ET process represents a key step for photonic-energy conversion in nanocrystalline solar cells.<sup>8,21</sup>

Employing femtosecond spectroscopy techniques, it has been demonstrated that electron-injection processes at dye-semiconductor interfaces often take place on an ultrafast time scale.<sup>6–12</sup> Electron injection as fast as 6 fs has been reported, e.g., for alizarin adsorbed on TiO<sub>2</sub> nanoparticles.<sup>11</sup> Studies of other dye molecules with electron-injection time scales of a few tens to a few hundred femtoseconds indicate that the coupling of the electronic dynamics to the nuclear (i.e., vibrational) motion of the chromophore may have a significant impact on the injection process.<sup>7,12</sup> As a result of this correlated electronic-nuclear dynamics, electron injection in these systems is not a simple exponential decay process and thus cannot be characterized by a single rate constant.

The theoretical study of interfacial ET processes requires a quantum mechanical description of the electron-injection dynamics including the coupling to the nuclear degrees of freedom. This has so far only been possible for models containing a single reaction coordinate<sup>14</sup> or within *ab initio* molecular dynamics simulations<sup>15,17,18</sup> employing classical approximations for the dynamics of the nuclei. In this Brief Report, we report results based on an accurate quantum mechanical treatment of the correlated electronic-nuclear dynamics including the multitude of nuclear degrees of freedom of the chromophore as well as the solvent environment. Furthermore, in extension of previous studies,<sup>16,19</sup> the interaction with the laser pulse is taken into account in a nonperturbative way, which allows an explicit description of the photoexcitation process that triggers the ET reaction. The explicit inclusion of the photoexcitation process in the theoretical description is particularly important for the systems

considered here because of the ultrafast time scale of the interfacial ET process.

To study the dynamics of ultrafast photoinduced electron injection from the electronically excited state of a chromophore into the conduction band of a semiconductor substrate, we consider a generic model of heterogeneous ET at surfaces based on an Anderson-Newns-type Hamiltonian.<sup>16,22</sup> The Hamiltonian is represented in a basis of the following diabatic (charge localized) electronic states: the electronic ground state of the overall system  $|\phi_g\rangle$ , the donor state of the ET process  $|\phi_d\rangle$  (which, in the limit of vanishing coupling between chromophore and semiconductor substrate, corresponds to the product of the first electronically excited state of the chromophore and an empty conduction band of the semiconductor), and the (quasi)continuum of acceptor states of the ET reaction  $|\phi_k\rangle$  (corresponding in the zero coupling limit to the product of the cationic state of the chromophore and an electron with energy  $\epsilon_k$  in the conduction band of the semiconductor substrate). Thus, the Hamiltonian describing the material reads

$$H_m = |\phi_g\rangle\epsilon_g\langle\phi_g| + |\phi_d\rangle\epsilon_d\langle\phi_d| + \sum_k |\phi_k\rangle\epsilon_k\langle\phi_k| + \sum_k (|\phi_d\rangle V_{dk}\langle\phi_k| + |\phi_k\rangle V_{kd}\langle\phi_d|) + H_n, \quad (1)$$

where  $H_n$  denotes the part of the Hamiltonian which involves the nuclear degrees of freedom.

The electronic coupling matrix elements  $V_{dk}$  and the distribution of energies  $\epsilon_k$  of the conduction band of the semiconductor can be specified by the energy-dependent decay width of the donor state  $\Gamma(E) = 2\pi\sum_k |V_{dk}|^2 \delta(E - \epsilon_k)$ . In the studies below, we have adopted a parametrization developed recently by Petersson *et al.*,<sup>23</sup>  $\Gamma(E) = \frac{2v_0(E-E_0)}{v^2} \{1 - [(E-E_0)^2 - \varepsilon^2 - 2v^2]/(2v^2)\}^{1/2}$ . The parameters describing the semiconductor substrate have been chosen to resemble injection into the lower 3d conduction band of TiO<sub>2</sub> ( $E_0 = -1.6$  eV,  $v = 2$  eV, and  $\varepsilon = 1.6$  eV). The overall coupling strength between chromophore and substrate  $v_0$  depends on the specific chromophore under consideration. For the system considered below (coumarin 343), a value of  $v_0 = 0.5$  eV has been determined based on experimental absorption spectra.<sup>19</sup>

To investigate the influence of the nuclear degrees of freedom on the ET reaction, we consider both the chromophore

and a solvent environment surrounding the dye-semiconductor system,  $H_n = H_c + H_s$ . The nuclear degrees of freedom of the chromophore are characterized using the normal modes of the electronic ground state as well as the gradients of the potential-energy surfaces of the first optically excited state and the ground state of the cation,

$$H_c = \frac{1}{2} \sum_l (P_l^2 + \Omega_l^2 Q_l^2) + \sum_l |\phi_d\rangle \kappa_l^d Q_l \langle \phi_d| + \sum_k |\phi_k\rangle \sum_l \kappa_l^a Q_l \langle \phi_k|. \quad (2)$$

The vibrational frequencies  $\Omega_l$  as well as the electronic-vibrational coupling constants  $\kappa_l^d$  and  $\kappa_l^a$  have been determined by electronic structure calculations employing density functional theory.<sup>24</sup>

To account for the influence of the surrounding solvent on the ET dynamics, we employ a standard (outer sphere) linear response model<sup>1,2</sup> where the Hamiltonian of the dye-semiconductor system is coupled to a bath of harmonic oscillators,

$$H_s = \frac{1}{2} \sum_j (p_j^2 + \omega_j^2 x_j^2) + |\phi_d\rangle \sum_j c_j^d x_j \langle \phi_d| + \sum_k |\phi_k\rangle \sum_j c_j^a x_j \langle \phi_k|. \quad (3)$$

The parameters of the solvent part of the Hamiltonian are characterized by the spectral densities  $J^d(\omega) = \frac{\pi}{2} \sum_j \frac{(c_j^d)^2}{\omega_j} \delta(\omega - \omega_j)$  and  $J^a(\omega) = \frac{\pi}{2} \sum_j \frac{(c_j^a)^2}{\omega_j} \delta(\omega - \omega_j)$  in the donor and acceptor states,<sup>25</sup> respectively.

The photoexcitation process is described by coupling the material to a laser field with Gaussian envelope function  $e(t)$ , carrier frequency  $\omega_L$  and full width at half maximum width  $\tau$ . The overall Hamiltonian thus reads  $H = H_m + H_f(t)$ , with  $H_f(t) = g(t)(|\phi_g\rangle \langle \phi_d| + |\phi_d\rangle \langle \phi_g|)$ ,  $g(t) = g_0 e^{-4 \ln^2(t/\tau)^2} \cos(\omega_L t)$ . The strength of the laser field  $g_0$  has been chosen to photoexcite 10% of the population of the ground state.

The electron-injection dynamics is described by the population of the donor state,

$$P_d(t) = \text{tr}\{\rho_n |\phi_d\rangle \langle \phi_d| U^\dagger(t) |\phi_d\rangle \langle \phi_d| U(t)\}, \quad (4)$$

where  $\rho_n$  denotes the initial state of the nuclear degrees of freedom (described by the respective Boltzmann operator at  $T=300$  K), and  $U(t)$  is the time evolution operator corresponding to the Hamiltonian of the overall (material+field) system  $H(t)$ .

The dynamical simulations have been performed employing the multilayer formulation<sup>26</sup> of the multiconfiguration time-dependent Hartree method.<sup>27</sup> This rigorous variational approach allows an accurate (in principle, numerically exact) description of the quantum dynamics of systems with many degrees of freedom. In the calculation, the continuum of electronic band states as well as the continuous distribution of solvent modes are discretized and represented by a finite number of states and modes, respectively.<sup>16,28</sup> The dynamics of the thus obtained finite system is treated numerically exactly.

As a representative example of interfacial ET processes, we consider electron injection in the dye-semiconductor system coumarin 343 (C343)-TiO<sub>2</sub>.<sup>29</sup> The results of the dynamical

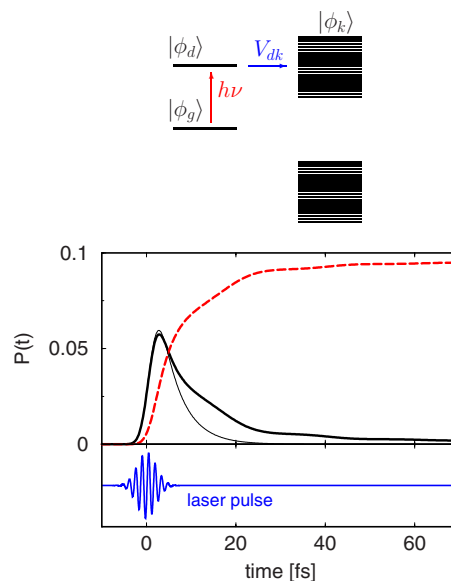


FIG. 1. (Color online) Photoinduced ET dynamics of the C343-TiO<sub>2</sub> system. Shown is the population of the donor (thick solid line) and acceptor (dashed line) states induced by a 5 fs laser pulse (lower panel). The thin solid line depicts the results of a purely electronic calculation. The upper panel gives a schematic illustration of the process.

simulation, depicted in Fig. 1, exhibit an ultrafast injection process. The photoexcitation of the donor state, induced by the ultrashort laser pulse ( $\tau=5$  fs), is followed by a decay into the conduction band of the semiconductor on a time scale of  $\approx 20$  fs. This time scale is at the lower boundary of experimental results for the C343-TiO<sub>2</sub> system, where injection times in the range of 20–200 fs have been found using different techniques.<sup>6,10,30</sup> In addition to the dominating ultrafast injection component, the simulation results also exhibit a small component with slower injection dynamics and a weak oscillatory structure superimposed on the decay. The comparison with a purely electronic calculation (where the coupling to the nuclear degrees of freedom has been neglected) reveals that both the slowly decaying component and the oscillatory structures are caused by the coupling of the electron to the nuclear degrees of freedom. Thereby, due to the ultrafast time scale of the injection, the major effect is caused by the intramolecular modes of C343.

To elucidate the underlying mechanism, we consider a simpler model case where only a single nuclear mode couples to the electronic degrees of freedom, schematically illustrated by the potential-energy surfaces in Fig. 2. The photoexcitation induced by the laser pulse prepares a nuclear wave packet in the Franck-Condon region of the potential-energy surface of the donor state. Because there are many crossings to the acceptor states in this region, the electron dynamics exhibits an ultrafast initial injection process. Due to the nonstationary preparation, however, the nuclei start to move along the gradient of the potential energy (illustrated by the nuclear wave packet in Fig. 2) and enter regions of configuration space with negligible overlap between donor and acceptor states, thus resulting in a small effective donor-acceptor coupling which causes a temporary trapping of the

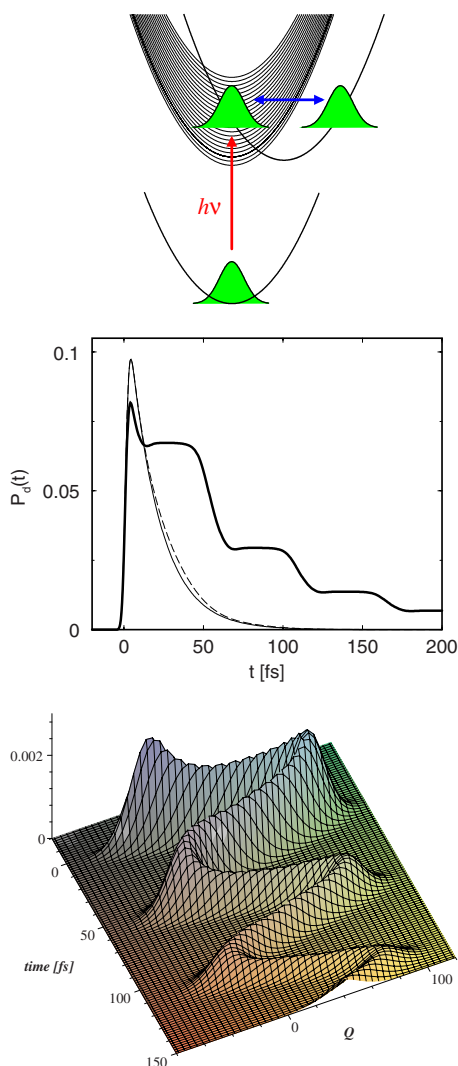


FIG. 2. (Color online) Photoinduced ET dynamics of a model system with potential-energy curves depicted in the upper panel. The middle panel depicts the population of the donor state induced by a 5 fs laser pulse. In addition to the results of accurate calculations (thick solid line), approximate results employing a mean-field method (thin dashed line) as well as purely electronic results (thin solid line) are shown. The lower panel depicts the vibrational wave packet in the donor state.

electron at the donor state. Upon return of the wave packet to the Franck-Condon region, the next ultrafast injection occurs, resulting in an overall steplike characteristics of the electron-injection dynamics. Thus, the correlated electronic-nuclear dynamics can be characterized as ET driven by coherent vibrational motion which results in slower electron-injection dynamics due to temporary trapping of the electron at the donor site.

In a real dye-semiconductor system, such as C343-TiO<sub>2</sub>, the dynamics is significantly more complex. A detailed analysis shows that different time scales of the vibrations may result in different electronic-nuclear dynamics for the C343-TiO<sub>2</sub> system. As in the one-dimensional model problem, the oscillatory structures superimposed on the electronic decay dynamics are caused by coupling to high-frequency vibrations. Such modes can influence the electronic dynam-

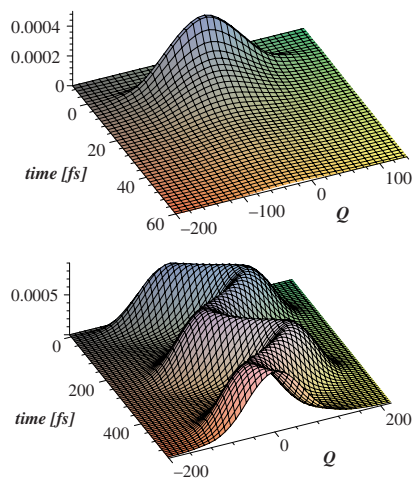


FIG. 3. (Color online) Wave-packet dynamics of a low-frequency vibrational normal mode of C343 after photoexcitation. Shown is the reduced density in the donor state (upper panel) and averaged over the acceptor states (lower panel), respectively.

ics directly because the vibrational period is similar to the electron-injection time scale. Low-frequency (slow) modes exhibit another interesting effect, as illustrated in Fig. 3, for the wave-packet motion of the vibration of the nitrogen group in C343 ( $\Omega=133\text{ cm}^{-1}$ ). This mode has negligible changes in equilibrium geometry with respect to photoexcitation but shows a rather large displacement with respect to the ET process, i.e., the transition from the photoexcited state to the cation. As a result, the photoexcitation prepares an (with respect to this mode) essentially stationary wave packet in the donor state. On the other hand, the wave packet in the acceptor states shows pronounced oscillatory motion. This motion is induced by the ultrafast ET process, the time scale of which ( $\approx 20\text{ fs}$ ) is more than one order of magnitude faster than the vibrational period of the mode ( $t=2\pi/\Omega \approx 251\text{ fs}$ ). Thus, the ultrafast ET process prepares a coherent wave packet on the potential-energy surface of the acceptor states, which then starts to oscillate. This process of ET-induced vibrational motion is beyond the traditional Marcus theory of ET,<sup>1</sup> which assumes that vibrational relaxation is faster than ET so that ET proceeds from a vibrationally relaxed initial state. Here, ET is so fast that it can induce coherent vibrational motion.

The details of the ET dynamics depend on the specific dye-semiconductor system. A particularly important parameter is the energetic location of the donor state relative to the conduction band edge  $\epsilon_d$ . In the C343-TiO<sub>2</sub> system, the energy of the donor state is 0.53 eV above the conduction band edge, thus facilitating an ultrafast and complete injection process. To illustrate the influence of this parameter, Fig. 4 shows the results of calculations for situations where the energy of the donor state is closer to the conduction band edge. The lower energy of the donor state results in qualitatively different dynamics. In particular, the decay into the conduction band of TiO<sub>2</sub> becomes slower and, for a sufficiently low value of  $\epsilon_d$ , incomplete; i.e., there is a finite probability that the electron is trapped at the chromophore, which has important consequences for the injection yield. The comparison

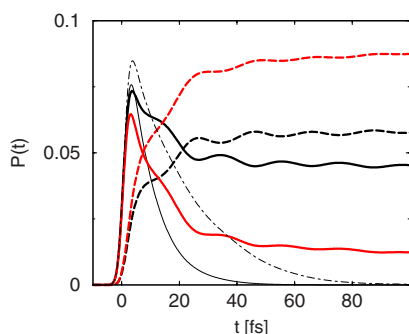


FIG. 4. (Color online) Influence of the location of the donor state (relative to the conduction band edge) on the injection dynamics. Shown is the population of the donor (thick solid lines) and acceptor (thick dashed lines) states for  $\epsilon_d=0.41$  eV (red and/or gray lines) and  $\epsilon_d=0.29$  eV (black lines), respectively. All other parameters are the same, as in Fig. 1. In addition, results of approximate calculations for the population of the donor state are shown for the case  $\epsilon_d=0.29$  eV. Thin solid lines depict results neglecting electronic-vibrational coupling, and thin dashed-dotted lines show results employing a mean-field approximation.

with results of purely electronic calculations indicates that this effect is induced by nuclear motion. A more detailed analysis reveals that the localization is caused by nuclear relaxation from the initial geometry (i.e., the equilibrium geometry of the ground state) into regions of configuration space close to the equilibrium geometry of the donor state, where the electronic Hamiltonian possesses bound eigenstates, and is thus a combined electronic-nuclear effect. This is further corroborated by the results of a mean-field calculation, which demonstrate that this localization effect can only be described correctly if electronic-nuclear correlation is properly taken into account.

The results of accurate quantum dynamical calculations presented above demonstrate the entanglement and mutual influence of electronic and nuclear dynamics in photoin-

duced heterogeneous ET reactions at dye-semiconductor interfaces. Depending on the relative time scale of electronic and nuclear dynamics, electronic-nuclear coupling may result in ET driven by coherent vibrational motion (for high-frequency modes) or vibrational motion induced by ultrafast ET (for low-frequency modes). These effects are particularly pronounced for dye-semiconductor systems with not too strong chromophore-substrate interaction and donor states close to the conduction band edge. In this case, electronic-nuclear coupling may, furthermore, cause localization of the electron at the chromophore, thus resulting in an incomplete electron-injection process. These findings may be instrumental for the optimization of the electron-injection process in nanocrystalline solar cells.

Finally, it should be noted that in the present Brief Report, we have used a simple semiempirical modeling of the semiconductor substrate and the chromophore-semiconductor coupling. This modeling is well suited for the study of generic mechanisms in interfacial ET processes. A more detailed atomistic description requires first-principles electronic structure calculations. Using atomistic models would also allow us to investigate the influence of the adsorption geometry of the chromophore on the ET dynamics. It is also noted that the dynamical methodology employed in the present Brief Report can also be used to study the influence of the shape of the laser pulse on the ET process. Both extensions of the present Brief Report will be the subject of future work.

We thank Wolfgang Domcke for helpful discussions. The generous allocation of computing time by the National Energy Research Scientific Computing Center and the Leibniz Rechenzentrum, Munich, is gratefully acknowledged. This work has been supported by the Deutsche Forschungsgemeinschaft (DFG) through the DFG-Cluster of Excellence, Munich Centre for Advanced Photonics and a research grant (M.T.) and the National Science Foundation (NSF) CAREER under Award No. CHE-0348956 (H.W.).

\*Present address: Forschungszentrum Karlsruhe, Herrmann-von-Helmholtz-Platz 1, 76344 Eggenstein-Leopoldshafen, Germany.

<sup>1</sup>R. A. Marcus, *Rev. Mod. Phys.* **65**, 599 (1993).

<sup>2</sup>V. May and O. Kühn, *Charge and Energy Transfer Dynamics in Molecular Systems* (Wiley-VCH, Weinheim, 2004).

<sup>3</sup>M. H. Vos *et al.*, *Proc. Natl. Acad. Sci. U.S.A.* **88**, 8885 (1991).

<sup>4</sup>P. F. Barbara *et al.*, *J. Phys. Chem.* **100**, 13148 (1996).

<sup>5</sup>M. Reed *et al.*, *Science* **278**, 252 (1997).

<sup>6</sup>J. M. Rehm *et al.*, *J. Phys. Chem.* **100**, 9577 (1996).

<sup>7</sup>C. Zimmermann *et al.*, *J. Phys. Chem. B* **105**, 9245 (2001).

<sup>8</sup>J. Asbury *et al.*, *J. Phys. Chem. B* **105**, 4545 (2001).

<sup>9</sup>J. Schnadt *et al.*, *Nature (London)* **418**, 620 (2002).

<sup>10</sup>R. Huber *et al.*, *Chem. Phys. Lett.* **285**, 39 (2002).

<sup>11</sup>R. Huber *et al.*, *J. Phys. Chem. B* **106**, 6494 (2002).

<sup>12</sup>G. Benkő *et al.*, *J. Am. Chem. Soc.* **124**, 489 (2002).

<sup>13</sup>B. Brüggemann *et al.*, *Phys. Rev. Lett.* **97**, 208301 (2006).

<sup>14</sup>S. Ramakrishna *et al.*, *Phys. Rev. B* **62**, R16330 (2000).

<sup>15</sup>W. Stier and O. V. Prezhdo, *J. Phys. Chem. B* **106**, 8047 (2002).

<sup>16</sup>M. Thoss *et al.*, *Chem. Phys.* **304**, 169 (2004).

<sup>17</sup>L. C. G. Rego *et al.*, *J. Chem. Phys.* **122**, 154709 (2005).

<sup>18</sup>C. F. Craig *et al.*, *Phys. Rev. Lett.* **95**, 163001 (2005).

<sup>19</sup>I. Kondov *et al.*, *J. Phys. Chem. A* **110**, 1364 (2006).

<sup>20</sup>P. Persson *et al.*, *J. Chem. Theory Comput.* **2**, 441 (2006).

<sup>21</sup>M. Grätzel, *Nature (London)* **414**, 338 (2001).

<sup>22</sup>D. News, *Phys. Rev.* **178**, 1123 (1969).

<sup>23</sup>A. Petersson *et al.*, *J. Phys. Chem. B* **104**, 8498 (2000).

<sup>24</sup>I. Kondov *et al.*, *Int. J. Quantum Chem.* **106**, 1291 (2006).

<sup>25</sup>The spectral densities of the solvent model,  $J^d(\omega) = \sqrt{\frac{\lambda_G \omega}{\pi}} e^{-[\omega/(2\omega_G)]^2} + 2\lambda_D \frac{\omega \omega_D}{\omega^2 + \omega_D^2}$ , and  $J^a(\omega) = \alpha^2 J^d(\omega)$ , and the corresponding parameters,  $\omega_G = 144 \text{ cm}^{-1}$ ,  $\omega_D = 25 \text{ cm}^{-1}$ ,  $\lambda_D^d = \lambda_G^d = 700 \text{ cm}^{-1}$ , and  $\alpha = -0.1$ , have been chosen in accordance with experimental results on solvation dynamics and absorption spectra of C343 in water (Refs. 10 and 31).

<sup>26</sup>H. Wang and M. Thoss, *J. Chem. Phys.* **119**, 1289 (2003).

<sup>27</sup>H.-D. Meyer *et al.*, *Chem. Phys. Lett.* **165**, 73 (1990).

<sup>28</sup>For the system considered in this Brief Report, 40 bath modes and 200 electronic states are required for convergence to the continuum limit on the time scale of interest.

<sup>29</sup>The details of the model and the model parameters are described in Ref. 19.

<sup>30</sup>H. N. Gosh *et al.*, *J. Phys. Chem. B* **102**, 10208 (1998).

<sup>31</sup>R. Jimenez *et al.*, *Nature (London)* **369**, 471 (1994).